Biophysical Journal, Volume 99

Supporting Material

Structural Determination of Aβ 25-35 Micelles by Molecular Dynamics Simulations

Xiang Yu, Qiuming Wang, and Jie Zheng

Structural Determination of $A\beta_{25-35}$ Micelles by Molecular Dynamics Simulations

XiangYu, Qiuming Wang, and Jie Zheng*
Department of Chemical & Biomolecular Engineering
The University of Akron, Akron, OH 44325

* To whom correspondence should be addressed: zhengj@uakron.edu

Running Title: $A\beta_{25-35}$ micelle structures

Keywords: amyloid, Aβ, micelle, and molecular dynamics

Explicit-solvent MD simulation protocol

The selected micelle structures were solvated in a TIP3P water cubic box of 80×80 ×80 $Å^3$ with a margin of at least 15 Å from any edge of the water box to any Aβ atom. Water molecules within 2.4 Å of the Aβ were removed. The systems were then neutralized by adding counter ions of Cl^- and Na^+ to reach ionic strength of ~120 mM. The resulting systems were minimized in energy for 5000 steps with peptides restrained, followed by additional 5000 steps of minimization for the whole system to remove unfavorable contacts between solvent and peptides. The systems were then subject to 1 ns MD run with harmonica constrained on the backbone atoms of the Aβs. The production runs were carried out in the NPT ensemble (1 atm and 300 K). Constant pressure (1 atm) and temperature (300 K) in the system were maintained by an isotropic Langevin barostat and a Langevin thermostat, respectively. Long-range electrostatics interactions were treated by the particle mesh Ewald sum method, while short-range van der Waals (VDW) interactions were evaluated by a switching method with a twin range cutoff of 10 and 12 Å. The integration time step was 2 fs with the RATTLE algorithm applied to constrain bonds involving hydrogen atoms. Periodic boundary condition with the minimum image convention was applied to all directions. All models were run twice to validate simulation convergence by using the same starting coordinates but different initial velocities assigned by the Maxwell-Boltzman distribution. All MD simulations were performed by the NAMD program (1) with all-atom CHARMM27 force field (2) on the Glenn cluster at the Ohio Supercomputer Center and our own Atom linux cluster. The summary of simulation systems were listed in Table 1.

Molecular docking

To identify the biological relevance of our micelle models, we docked all six micelles to antibody (PDB: 3BAE) (3) by using Patchdock (4) and Firedock (5). Each Aβ micelle was first coarsely docked to the F_{ab} regions of antibody by using the PatchDock that only allows the interface residues to be flexible. The top 150 Aβ-IgG complexes within the clustering RMSD of 4 Å were then subject to the FireDock to optimize the Aβ-IgG interactions by allowing the rigid-body adjustment and the flexible backbone and sidechain movements between Aβ and IgG. The refined Aβ-IgG complexes from the FireDock simulations yield better binding energy and hardly include steric clashes. The best-hit complex were shown in Figure 5.

Data Analysis

(i) Conformational stability of the micelle is measured by backbone root mean square deviation (RMSD) relative to the initial energy-minimized structure throughout the simulations. (ii) Overall size of a micelle is measured by radius of gyration (Rg). Rg is defined as the mass-weighted geometric mean of the distance of each atom from the micelle's center of mass. (iii) A hydrogen bond is identified if the distance between donor D and acceptor A is < 3.5 Å and the angle D-H···A is > 120°, while a sidechain contact is defined when the mass center distance between a pair of sidechains is < 6.5 Å.

Table S1. Structural characterization for six micelles

Systems	Φ (°)	λ (Å)	Backbone RMSD (Å)	Rg (Å)	Time (ns) and # of runs
P_N	210	1.6	10.5	27.2	8, 2
P_C	45	0	11.5	28.1	8, 2
AP_N	255	0.8	7.2	24.5	44, 2
AP_C	60	0.4	8.3	24.9	44, 2
AP_N_K28A	255	0.8	7.1	23.8	44, 2
AP_C_K28A	60	0.4	6.7	23.6	44, 2

RMSD and Rg are averaged from the last 4 nanosecond.

Table S2. Surface hydrophobicity characterized by solvent accessible solvent surface. SASA data were averaged from the last 4-ns of each simulation.

Systems	Hydrophobic SASA (Å^2)	Hydrophilic SASA (Å^2)	Charged SASA (Å^2)
P_N	12776 ± 213	18655 ± 281	6056 ± 118
P_C	23002 ± 316	14575 ± 303	5559 ± 244
AP_N	13197 ± 234	13173 ± 271	5132 ± 185
AP_C	15529 ± 352	12098 ± 222	5783 ± 110
AP_N_K28A	14783 ± 319	12462 ± 268	0
AP_C_K28A	16327 ± 317	11088 ± 205	0

Table S3. Self-diffusion coefficient (D) of waters near the micelles and in bulk solution. Interfacial waters are defined by a separation distance of 6 Å within the outermost heavy atoms of the micelles.

System	D ($\times 10^{-5}$ cm^2/s)
P_N	0.116
P_C	0.334
AP_N	0.332
AP_C	0.778
AP_N_K28A	0.137
AP_C_K28A	0.610

Figure S1. Monomeric $A\beta_{25-35}$ peptide with a large hydrophobic C-terminals and a small polar N-terminal, exhibits α-helical structure. Hydrophobic residue (red), polar residue (green), and positively charged residue (blue).

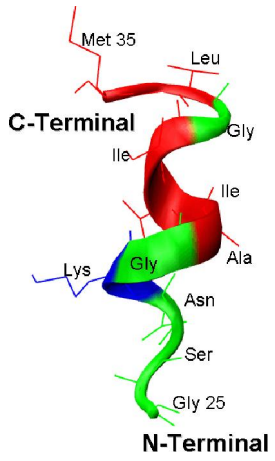

Figure S2. Energy landscapes projected onto peptide self-rotation along the helical axis and peptide displacement between different layers for (a) P_N, (b) P_C, (c) AP_N, and (d) AP_C categories. Four lowest-energy Aβ micelles, each from one category, are selected from 504 candidates and identified by red cycles.

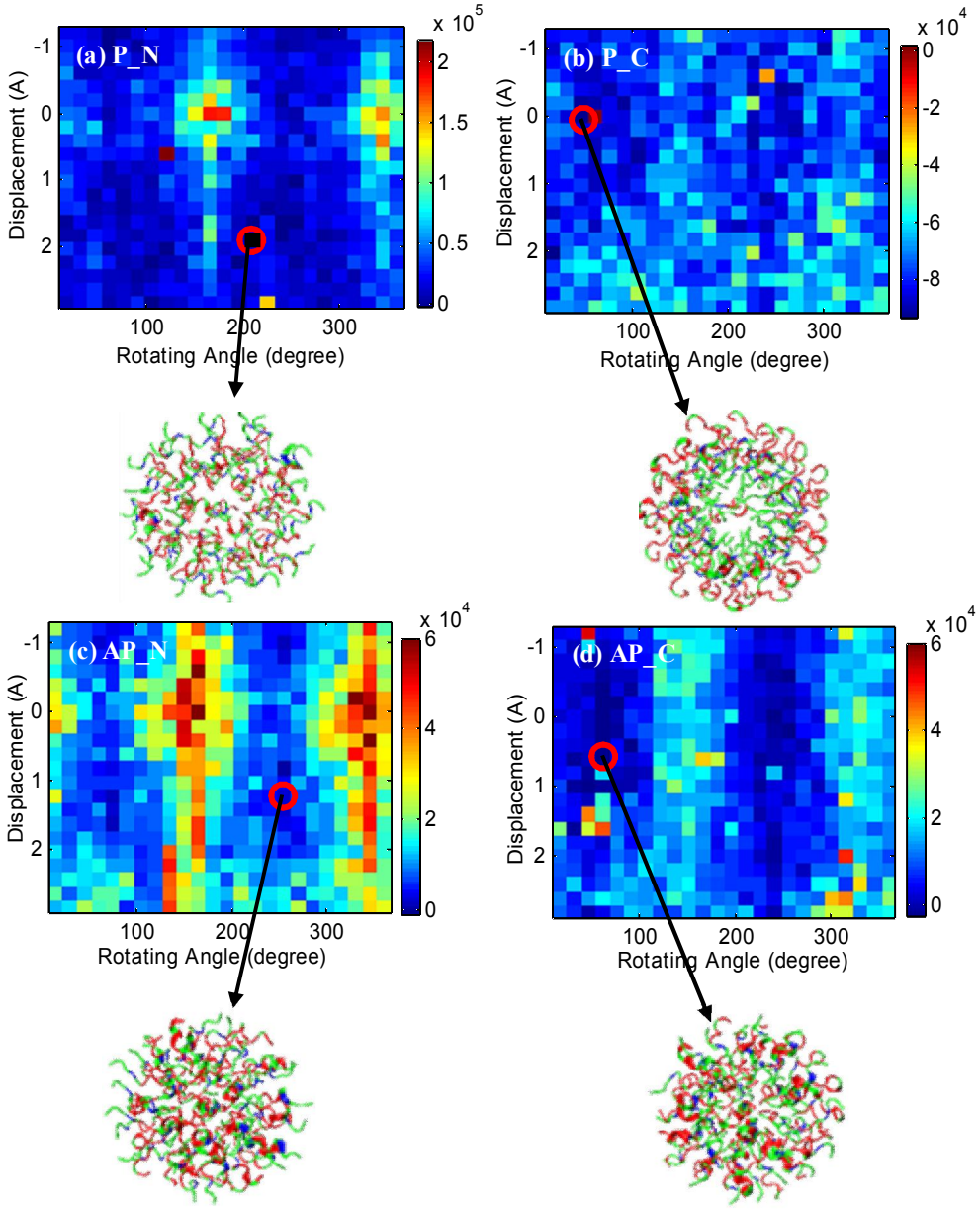

Figure S3. Structural characteristics and comparison for all micelles. (a-b) time evolution of backbone RMSD and radius of gyration of micelles. (c) residue-based backbone RMSF for Aβ monomers averaged from each micelle.

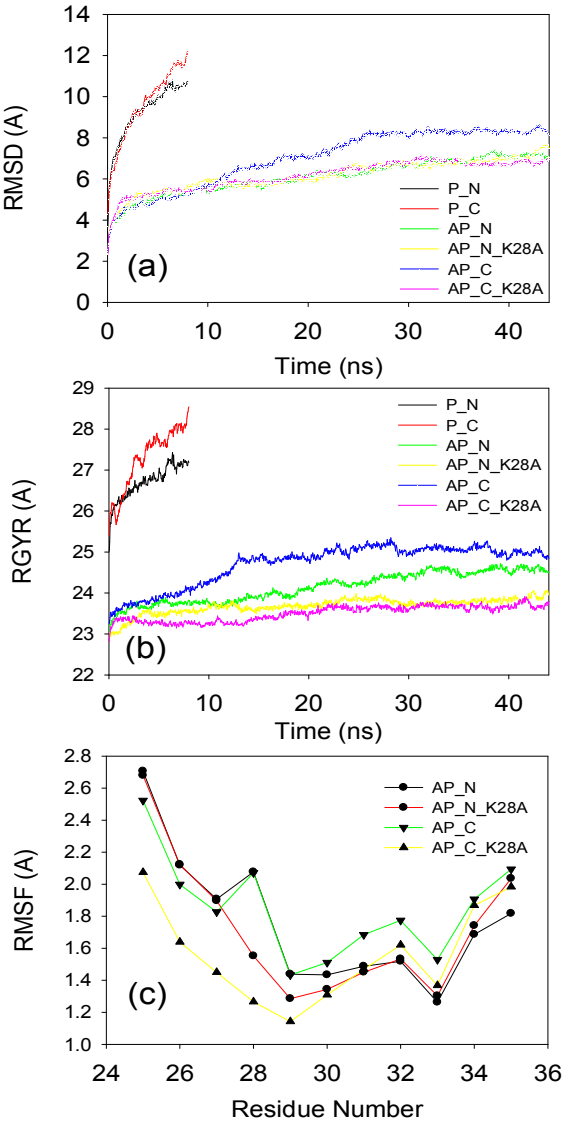

Figure S4. MD snapshots for the P_N, P_C, AP_N, AP_C, AP_N_K28A, and AP_C_K28A micelles. Two micelles of P_N and P_C with parallel peptide orientation are unstable, while other four micelles with antiparallel peptide orientation are stable within 44 ns. Hydrophobic residue (red), polar residue (green), and positively charged residue (blue).

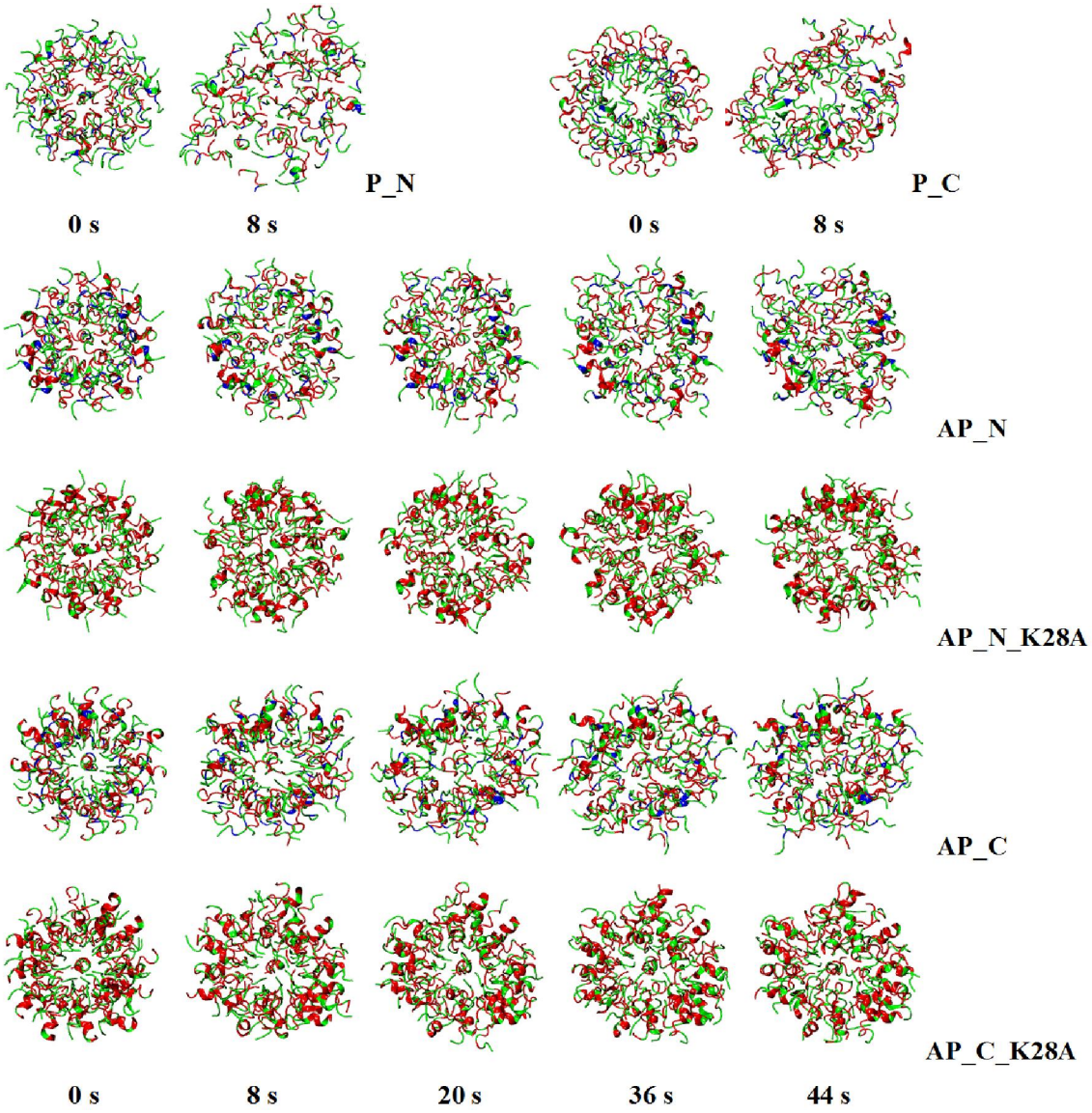

Figure S5. MD snapshots for additional two parallel micelles and two antiparallel micelles, which are selected from energy landscape in Figure S2. Consistently, both antiparallel structures displayed similar high structural stability within 40 ns, while parallel structures transformed into non-spherical shapes within 8 ns.

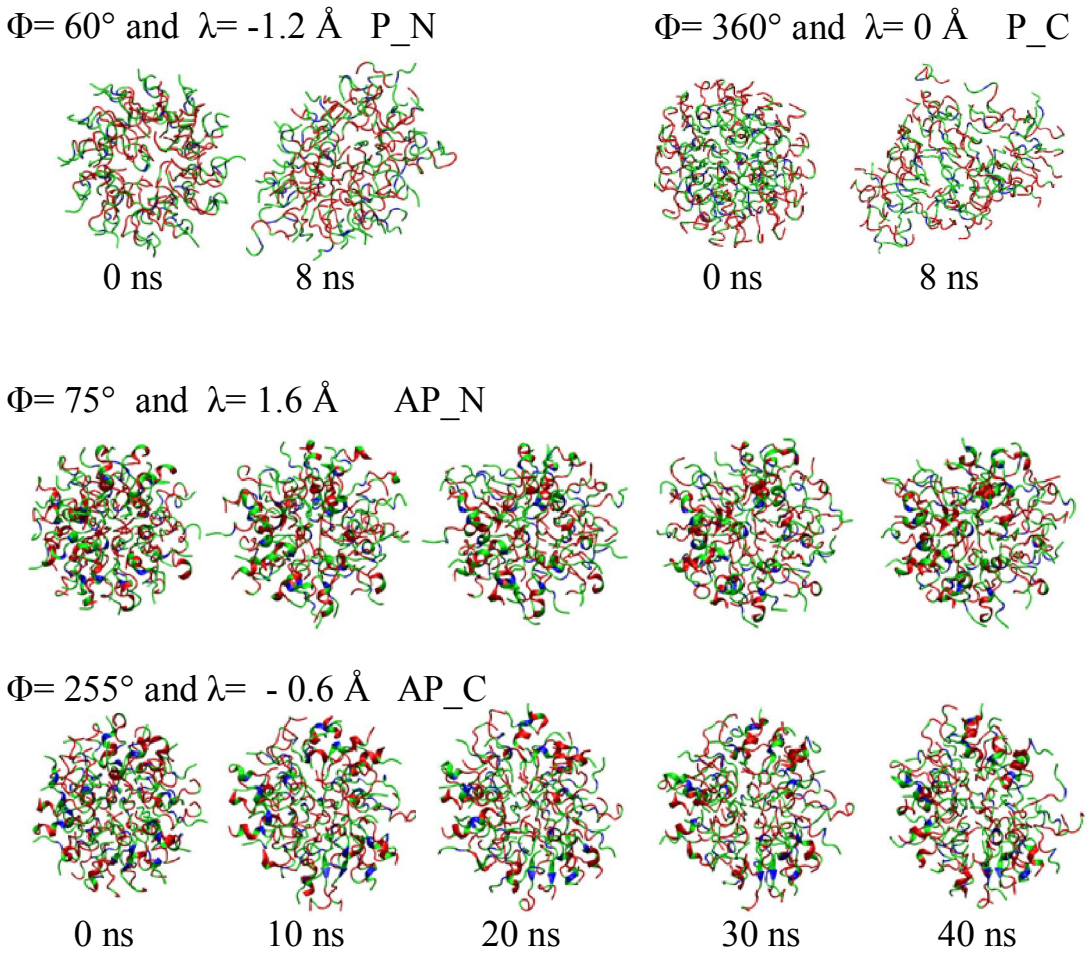

1. Kale, L., R. Skeel, M. Bhandarkar, R. Brunner, A. Gursoy, N. Krawetz, J. Phillips, A. Shinozaki, K. Varadarajan, and K. Schulten. 1999. NAMD2: Greater scalability for parallel molecular dynamics. Journal of Computational Physics 151:283-312.
2. Brooks, B. R., R. E. Bruccoleri, B. D. Olafson, D. J. States, S. Swaminathan, and M. Karplus. 1983. Charmm - a Program for Macromolecular Energy, Minimization, and Dynamics Calculations. Journal of Computational Chemistry 4:187-217.
3. Miles, L. A., K. S. Wun, G. A. N. Crespi, M. T. Fodero-Tavoletti, D. Galatis, C. J. Bagley, K. Beyreuther, C. L. Masters, R. Cappai, W. J. McKinstry, K. J. Barnham, and M. W. Parker. 2008. Amyloid-[beta]-anti-amyloid-[beta] complex structure reveals an extended conformation in the immunodominant B-Cell epitope. J. Mol. Biol. 377:181-192.
4. Schneidman-Duhovny, D., Y. Inbar, R. Nussinov, and H. J. Wolfson. 2005. PatchDock and SymmDock: servers for rigid and symmetric docking. Nucl. Acids Res. 33:W363-367.
5. Mashiach, E., D. Schneidman-Duhovny, N. Andrusier, R. Nussinov, and H. J. Wolfson. 2008. FireDock: a web server for fast interaction refinement in molecular docking. Nucl. Acids Res. 36:W229-232.